

# Controlling Complex Fractional Order Systems with the PID Controller

Bilal Şenol<sup>1\*</sup>, Emre Avuçlu<sup>1</sup> and Uğur Demiroğlu<sup>2</sup>

<sup>3</sup>Aksaray University, Department of Software Engineering, Aksaray, Türkiye

<sup>2</sup>İnönü University, Department of Computer Engineering, Malatya, Türkiye

\*bilal.senol@aksaray.edu.tr

**Abstract** – This paper focuses on the Fractional Complex Order Plant (FCOP) plant model, which has recently acquired favor in applied physics and control systems. The consideration of the physical phenomena of complex plant models and how they impact the stability and durability of the systems is the main addition of this recommended research to the literature. Because the FCOP plant model is the most generic mathematical form, covering the Integer Order Plant (IOP) and Fractional Order Plant (FOP) models, other plant models may be readily developed with this benefit. The physical changes of the computational equations produced with the proposed approach and the suggested IOPI controller are seen for fractional complex order plants. The effects of the factors on the system are investigated alongside simulation values. For the plant type, the benefits and drawbacks of the chosen controller setup can also be discussed.

**Keywords** – Fractional Complex Order, Fractional Order, Integer Order, Proportional Integral Derivative, Controller Design, Analytical Method

## I. INTRODUCTION

Control system design has a very important place in the industry. The controller modeled for real processes is required to be simple, most cost-effective and meet all constraints. Controller parameters must be designed to meet these requirements and operate at various values. During the design process, the stability and durability of the system were among the most important goals to be achieved. In addition to stability and robustness, it would be useful to consider the widest frequency range in which the system can operate when designing the controller.

The controllers will have a major task in ensuring that the complex and energy-intensive control systems in real industrial processes operate in a dependable and efficient manner [1]. Numerous contemporary industrial applications make use of proportional-integrative-derivative (PID) controllers [2]-[4]. The PID technique is widely used in process control in industry [5]. Sadly, long-term memory effects—which are found in many other complex systems linked to processes with non-local dynamics—are absent from PID

controllers. Fractional calculus can be used for higher-accuracy modeling, for example, for arbitrary-order integration and differentiation [6], [7]. A typical PID model used for control purposes is based on integer order calculus, and integer derivative operators do not have the non-locality property [8], [9]. Ziegler and Nichols designed one of the most well-known vehicle tuning methods [10]. It may be used to a wide range of study fields, such as neural networks, signal processing, thermal diffusion, chaotic systems, viscoelasticity, and mechatronic systems [11]-[17]. It is an essential instrument for providing a detailed description of real-world physical processes. For example, a hydraulic servo system with substantial mechanical inertia and historical dependency has been controlled using the fractional-order derivative [18]. Furthermore, fractional calculus has been heavily utilized in both system modeling and controller design investigations [19]-[22].

In order to produce analytical solutions and explore the underlying physical phenomena, this study makes use of the Fractional Complex Order Plant (FCOP) plant model and PID controller

structure, which are increasingly used in applied physics and control systems. We consider a complex system whose controller structure hasn't gotten much attention in the literature up to this time. Simulations and images are used to describe and provide support for the results of the solutions generated with varying parameter values for the system's stability and durability. When building a system, the effects of the real and imaginary components of the complex number are considered differently.

For fractional order plants, the first study about the concept was built up in 2019 [23]. Then, with developments, the theory was further improved [24]-[26].

This paper is organized in the following way. The second section gives information about the closed loop and open loop system integration. The third section gives the design procedure of the FCOP.

## II. SYSTEM INTEGRATION

The block diagram of the closed loop control system used in this study is shown in Fig. 1.

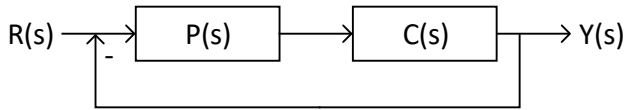


Fig. 1. A closed loop control system

The system's Laplace sign input is  $R(s)$ , and its Laplace sign output is  $Y(s)$ . The regulated system is indicated by  $P(s)$ , and the controller that will control the system is indicated by  $C(s)$ .  $G(s)$ , the system's open loop transfer function, may be calculated as below.

$$R(s)P(s)C(s) = Y(s) \Rightarrow G(s) = \frac{Y(s)}{R(s)} = P(s)C(s) \quad (1)$$

The system's closed-loop transfer function, or  $T(s)$ , may be obtained with the following equation.

$$(R(s) - Y(s))P(s)C(s) = Y(s) \Rightarrow T(s) = \frac{Y(s)}{R(s)} = \frac{P(s)C(s)}{1 + P(s)C(s)} = \frac{G(s)}{1 + G(s)} \quad (2)$$

It is evident that there is a close relationship between the system's open-loop and closed-loop transfer functions [24], [25].

The combined amplitude and phase margin graphs of the system are displayed in the Bode diagram, a type of graph used in system analysis. It is quite helpful to have two system components in one picture at the same time. Bode diagrams are used in open loop systems analysis. The first part of the system is the amplitude margin, which indicates how much the gain of the open loop system may be raised to guarantee system stability. The second component of the system is the phase margin, which defines the maximum phase increase that the open loop system may undergo to maintain system stability [23], [26].

In the Bode diagram, the phase crossover frequency is  $\omega_{gc}$  and the gain crossover frequency is  $\omega_{pc}$ . In contrast, the frequency at which the amplitude graph's slope crosses 0dB is known as the gain crossover frequency. Phase crossover frequency is the frequency value at the location on the phase graph where the curve cuts  $-180^\circ$ .

In the Bode diagram, it is defined as the GM amplitude margin and the PM phase margin. The distance between the phase value at frequency  $\omega_{gc}$  and  $-180^\circ$  on the phase graph, respectively, is known as the phase margin. The amplitude margin on the amplitude graph is the distance of the amplitude value at frequency  $\omega_{pc}$  from 0dB.

The gain crossover frequency requirements for the Bode diagram that will be utilized in this inquiry are provided by the following presentations.

$$\angle G(s) \Big|_{s=j\omega_{gc}} = PM - \pi \quad (3)$$

$$|G(s)| \Big|_{s=j\omega_{gc}} = 1 \quad (4)$$

Similarly, the phase crossover frequency requirements for the Bode diagram that will be utilized in this study are provided as follows.

$$\angle G(s) \Big|_{s=j\omega_{pc}} = -\pi \quad (5)$$

$$|G(s)| \Big|_{s=j\omega_{pc}} = 10^{GM/20} \quad (6)$$

It is evident that the stability and durability of the system over a wide range are strongly correlated with the gain and phase crossover frequencies of the bode diagram.

### III. DESIGNING THE PLANT

With exponential, time-delayed, or non-delayed additional gain coefficients, as well as integer, fractional, and complex number coefficients, the following is the most generic plant in a transfer function that may be encountered.

$$P(s) = K \frac{\sum_{i=0}^m (ae_i + jao_i) s^{(\alpha e_i + j\alpha o_i)}}{\sum_{k=0}^n (be_k + jbo_k) s^{(\beta e_k + j\beta o_k)}} e^{-Ls} \quad (7)$$

The time delay coefficients are  $L$ , and the gain is  $K$ . In the most generic version of the plant that has been proposed, the  $i^{\text{th}}$  even component of the complex coefficients of the  $m+1$  polynomial numerator is represented by  $ae_i$ , whereas the  $i^{\text{th}}$  odd portion is represented by  $ao_i$ .  $be_k$  represents the  $k^{\text{th}}$  odd component of the complex coefficients of the  $n+1$  polynomial denominators in the suggested structure, while  $bo_k$  represents the  $k^{\text{th}}$  even part.

The  $i^{\text{th}}$  even component is represented by  $\alpha e_i$ , whereas the  $i^{\text{th}}$  odd part of the complex exponents of the  $m+1$  polynomial numerator is represented by  $\alpha o_i$ .  $\beta o_k$  represents the  $k^{\text{th}}$  odd component and  $\beta e_k$  represents the  $k^{\text{th}}$  even portion of the complex exponents of the  $k+1$  polynomial denominator in the most generic form that has been presented.

The following transfer function indicates the most general form of the plant frequency response.

$$P(j\omega) = K \frac{\sum_{i=0}^m (j\omega)^{\alpha e_i + j\alpha o_i} (ae_i + jao_i)}{\sum_{k=0}^n (j\omega)^{\beta e_k + j\beta o_k} (be_k + jbo_k)} e^{-L(j\omega)} \quad (8)$$

By converting a complex number from exponential to trigonometric and back again, using Euler's Equation, the numerator of the plant frequency response may be easily expressed, as follows.

$$(j\omega)^{\alpha e_i + j\alpha o_i} = e^{-\frac{\pi\alpha o_i}{2}} \omega^{\alpha e_i} \begin{pmatrix} \cos\left(\frac{\pi\alpha e_i}{2} + \log(\omega)\alpha o_i\right) + \\ j \sin\left(\frac{\pi\alpha e_i}{2} + \log(\omega)\alpha o_i\right) \end{pmatrix} \quad (9)$$

Similarly, the transformation of the denominator polynomial's complex order is represented by the following equation.

$$(j\omega)^{\beta e_k + j\beta o_k} = e^{-\frac{\pi\beta o_k}{2}} \omega^{\beta e_k} \begin{pmatrix} \cos\left(\frac{\pi\beta e_k}{2} + \log(\omega)\beta o_k\right) + \\ j \sin\left(\frac{\pi\beta e_k}{2} + \log(\omega)\beta o_k\right) \end{pmatrix} \quad (10)$$

The above formulae can then be changed to exponential form in order to re-express the plant frequency response as,

$$P(j\omega) = K \frac{\sum_{i=0}^m e^{-\frac{\pi\alpha o_i}{2}} \omega^{\alpha e_i} e^{j\left(\frac{\pi\alpha e_i}{2} + \log(\omega)\alpha o_i\right)} (ae_i + jao_i)}{\sum_{k=0}^n e^{-\frac{\pi\beta o_k}{2}} \omega^{\beta e_k} e^{j\left(\frac{\pi\beta e_k}{2} + \log(\omega)\beta o_k\right)} (be_k + jbo_k)} e^{-jL\omega}. \quad (11)$$

The simple form of the plant frequency response given above is,

$$P(j\omega) = K \frac{(ne + jno)}{(de + jdo)} e^{-jL\omega} \quad (12)$$

The  $ne$  even component and  $no$  odd part of the numerator that makes up the frequency response of the plant are provided in the following equation.

$$ne = \sum_{i=0}^m e^{-\frac{\pi\alpha o_i}{2}} \omega^{\alpha e_i} \begin{pmatrix} \cos\left(\frac{\pi\alpha e_i}{2} + \log(\omega)\alpha o_i\right) ae_i - \\ \sin\left(\frac{\pi\alpha e_i}{2} + \log(\omega)\alpha o_i\right) ao_i \end{pmatrix} \quad (13)$$

$$no = \sum_{i=0}^m e^{-\frac{\pi\alpha o_i}{2}} \omega^{\alpha e_i} \begin{pmatrix} \sin\left(\frac{\pi\alpha e_i}{2} + \log(\omega)\alpha o_i\right) ae_i + \\ \cos\left(\frac{\pi\alpha e_i}{2} + \log(\omega)\alpha o_i\right) ao_i \end{pmatrix} \quad (14)$$

The  $de$  even and  $do$  odd parts of the denominator that make up the frequency response of the plant are provided as follows.

$$de = \sum_{k=0}^n e^{-\frac{\pi\beta o_k}{2}} \omega^{\beta e_k} \begin{pmatrix} \cos\left(\frac{\pi\beta e_k}{2} + \log(\omega)\beta o_k\right) be_k - \\ \sin\left(\frac{\pi\beta e_k}{2} + \log(\omega)\beta o_k\right) bo_k \end{pmatrix} \quad (15)$$

$$do = \sum_{k=0}^n e^{-\frac{\pi\beta o_k}{2}} \omega^{\beta e_k} \begin{pmatrix} \sin\left(\frac{\pi\beta e_k}{2} + \log(\omega)\beta o_k\right) be_k + \\ \cos\left(\frac{\pi\beta e_k}{2} + \log(\omega)\beta o_k\right) bo_k \end{pmatrix} \quad (16)$$

The frequency response of the plant in its most generic form, as determined by complex number

theory, is expressed in terms of its amplitude and phase values as follows.

$$P(j\omega) = |P(j\omega)|e^{j\angle P(j\omega)} \quad (17)$$

As a result, the following gives the amplitude value of the plant frequency response.

$$|P(j\omega)| = K \sqrt{\frac{ne^2 + no^2}{de^2 + do^2}} \quad (18)$$

Similarly, the following gives the phase value of the plant frequency response.

$$\angle P(j\omega) = \arctan\left(\frac{no}{ne}\right) - \arctan\left(\frac{do}{de}\right) - L\omega \quad (19)$$

Consequently, the formulas for calculating the amplitude and phase of the frequency response of the plant were discovered in their most general form. For the next step, frequency representations of the PID controller including the gain and the phase should be obtained. Then, the system's frequency response could easily be obtained by using the equations of the plant and the controller together. The further equations could be derived in this direction.

#### IV. CASE STUDY

This section gives an example to verify the proposed method.

Consider the following FCOP.

$$P(s) = \frac{1}{s^{1.25}j^{0.25} + 1} e^{-0.1s} \quad (20)$$

$\omega_{gc} = 5$  rad/s is considered as the optimal gain crossover frequency in this instance once more. Table 1 shows the parameters of the PID controller for varying values of the phase margin relative to the negative imaginary component.

Table 1. Parameters of the PID controller for varying values of PM relative to the negative imaginary component

| PM  | $\omega_{gc}$ | $\omega_{pc}$ | GM        | $k_p$    | $k_i$   | $k_d$    |
|-----|---------------|---------------|-----------|----------|---------|----------|
| 30° | 5             | 29.4660       | -16.92980 | 8.87967  | 44.5844 | 0.442131 |
| 35° | 5             | 30.3105       | -15.76230 | 9.43037  | 42.5858 | 0.522074 |
| 40° | 5             | 31.0037       | -14.66440 | 9.90929  | 40.4748 | 0.606513 |
| 45° | 5             | 31.5851       | -13.64010 | 10.31280 | 38.2676 | 0.694804 |
| 50° | 5             | 32.0817       | -12.68820 | 10.63780 | 35.9807 | 0.786277 |
| 55° | 5             | 32.5124       | -11.80570 | 10.88190 | 33.6318 | 0.880234 |
| 60° | 5             | 32.8907       | -10.98900 | 11.04310 | 31.2387 | 0.975961 |

In a similar way, Table 2 gives the parameters of the PID controller considering the positive imaginary component.

Table 2. Parameters of the PID controller for varying values of PM relative to the negative imaginary component

| PM  | $\omega_{gc}$ | $\omega_{pc}$ | GM       | $k_p$   | $k_i$   | $k_d$    |
|-----|---------------|---------------|----------|---------|---------|----------|
| 30° | 5             | 15.0538       | -7.74174 | 4.37395 | 10.0156 | 0.477540 |
| 35° | 5             | 15.6042       | -7.33345 | 4.32379 | 9.0663  | 0.515516 |
| 40° | 5             | 16.0862       | -6.92938 | 4.24072 | 8.1314  | 0.552909 |
| 45° | 5             | 16.5148       | -6.53993 | 4.12538 | 7.2182  | 0.589436 |
| 50° | 5             | 16.9005       | -6.17129 | 3.97864 | 6.3337  | 0.624819 |
| 55° | 5             | 17.2516       | -5.82719 | 3.80162 | 5.4844  | 0.658788 |
| 60° | 5             | 17.5739       | -5.50991 | 3.59567 | 4.6770  | 0.691086 |

This result indicates that the complex number degree plant is inversely proportional to the positive imaginary component and directly affects the system's phase crossover frequency, in contrast to fractional number degree plants.

#### V. CONCLUSION

This study focuses on the most exact analysis of physical changes and favors the plant model with the most general structure, in contrast to studies in the literature. To do this, it is preferable to utilize an IOPID controller to govern plant models for fractional order plants (FOP), fractional complex order plants (FCOP), and integer order plants (IOP). In addition, calculation formulae for the stability and durability of the system are produced utilizing the limitations of the Bode diagram. Simultaneously, the response of the system to unanticipated load disturbance signals was examined. Ultimately, results and illustrations from each of the three application cases were generated in the identical conditions, and a debate over the relative strengths of the systems and how they should be physically interpreted took place. Although many studies in the literature employ both full and fractional number-based plants, we think our proposed study will cover all system types. Because the calculation equations are readily found in the complex topic of the study, our arguments and findings have the potential to be novel. As the resulting parameters are altered, it is expected that new physical behaviours would emerge and be evaluated in future studies.

## REFERENCES

- [1] T. Xia, Z. Zhang, Z. Hong and S. Huang, "Design of fractional order PID controller based on minimum variance control and application of dynamic data reconciliation for improving control performance," *ISA Transactions*, vol. 133, pp. 91-101, 2022.
- [2] C. I. Muresan and R. De Keyser, "Revisiting Ziegler–Nichols. A fractional order approach," *ISA Transactions*, vol. 129, pp. 287-296, 2022.
- [3] Y. Chen, C. Hu, and K. L. Moore, "Relay feedback tuning of robust PID controllers with iso-damping property," in *42nd IEEE international conference on decision and control*, 2003.
- [4] K. J. Åström and T. Hägglund, "Revisiting the Ziegler–Nichols step response method for PID control," *Journal of process control*, 14(6), pp. 635-650, 2004.
- [5] A. A. Jamil, W. F. Tu, S. W. Ali, Y. Terriche and J. M. Guerrero, "Fractional-Order PID Controllers for Temperature Control: A Review," *Energies*, vol. 15(10), pp. 3800, 2022.
- [6] A. Kochubei and Y. Luchko, *Fractional differential equations*, Walter de Gruyter GmbH & Co KG, 2019.
- [7] C. A. Monje, Y. Q. Chen, B. M. Vinagre, D. Xue and V. Feliu-Batlle, *Fractional-order systems and controls: fundamentals and applications*, Springer Science & Business Media, 2010.
- [8] Y. Q. Chen and K. L. Moore, "Discretization schemes for fractional-order differentiators and integrators," *IEEE Transactions on Circuits and Systems I: Fundamental Theory and Applications*, vol. 49(3), pp. 363-367, 2002.
- [9] Ü. Lepik and H. Hein, *Fractional Calculus*, in Haar Wavelets Springer. pp. 107-122, 2014.
- [10] J. G. Ziegler and N. B. Nichols, "Optimum settings for automatic controllers," *trans. ASME*, vol. 64(11), 1942.
- [11] X. Li and L. Gao, "A Simple Frequency-domain Tuning Method of Fractional-order PID Controllers for Fractional-order Delay Systems," *International Journal of Control, Automation and Systems*, pp. 1-10, 2022.
- [12] A. Maachou, R. Malti, P. Melchior, J. Battaglia and B. Hay, "Thermal system identification using fractional models for high temperature levels around different operating points," *Nonlinear Dynamics*, vol. 70(2) pp. 941-950, 2012.
- [13] S. Luo, F. L. Lewis, Y. Song and K. G. Vamvoudakis, "Adaptive backstepping optimal control of a fractional-order chaotic magnetic-field electromechanical transducer," *Nonlinear Dynamics*, vol. 100(1), pp. 523-540, 2020.
- [14] E. Loghman, A. Kamali, F. B. Nejad and M. Abbaszadeh, "Nonlinear free and forced vibrations of fractional modeled viscoelastic FGM micro-beam," *Applied Mathematical Modelling*, vol. 92, pp. 297-314, 2021.
- [15] J. Shi, J. Zheng, X. Liu, W. Xiang and Q. Zhang, "Novel short-time fractional Fourier transform: theory, implementation, and applications," *IEEE Transactions on Signal Processing*, vol. 68, pp. 3280-3295, 2020.
- [16] Y. Wang, H. Zhong and B. Wang, "Fractional order model of three-winding series-connected single-phase motor," in *20th International Conference on Electrical Machines and Systems (ICEMS)*, 2017.
- [17] P. Liu, Z. Zeng and J. Wang, "Asymptotic and finite-time cluster synchronization of coupled fractional-order neural networks with time delay," *IEEE Transactions on Neural Networks and Learning Systems*, vol. 31(11): pp. 4956-4967, 2020.
- [18] P. Chen, B. Wang, Y. Tian and Y. Yang, "Finite-time stability of a time-delay fractional-order hydraulic turbine regulating system," *IEEE Access*, vol. 7, pp. 82613-82623, 2019.
- [19] L. Bai and D. Xue, "Universal block diagram based modeling and simulation schemes for fractional-order control systems," *ISA transactions*, vol. 82, pp. 153-162, 2018.
- [20] D. Li, L. Wei, T. Song and Q. Jin, "Study on asymptotic stability of fractional singular systems with time delay. International Journal of Control," *Automation and Systems*, vol. 18(4), pp. 1002-1011, 2020.
- [21] D. Li, X. He, T. Song and Q. Jin, "Fractional order IMC controller design for two-input-two-output fractional order system," *International Journal of Control, Automation and Systems*, vol. 17(4), pp. 936-947, 2019.
- [22] V. Feliu-Batlle, R. Rivas-Perez and F. J. Castillo-García, "Simple fractional order controller combined with a Smith predictor for temperature control in a steel slab reheating furnace," *International Journal of Control, Automation and Systems*, vol. 11(3), pp. 533-544, 2013.
- [23] B. Şenol and U. Demiroğlu, "Frequency frame approach on loop shaping of first order plus time delay systems using fractional order PI controller," *ISA Transactions*, vol. 86, pp. 192-200, 2019.
- [24] B. Şenol and U. Demiroğlu, "Fractional order proportional derivative control for first order plus time delay plants: achieving phase and gain specifications simultaneously," *Transactions of the Institute of Measurement and Control*, vol. 41(15), pp. 4358-4369, 2019.
- [25] B. Şenol, U. Demiroğlu and R. Matušů, "Fractional order proportional derivative control for time delay plant of the second order: The frequency frame," *Journal of the Franklin Institute*, vol. 357(12), pp. 7944-7961, 2020.
- [26] U. Demiroğlu and B. Şenol, "Frequency frame approach on tuning FOPI controller for TOPTD thermal processes," *ISA Transactions*, vol. 108, pp. 96-105, 2021.